Detection of Symmetry and Anti-Symmetry: What they Might Reveal about Visual Nonlinearities

Sandra Mancini

A Thesis

In

The Department

Of

Psychology

Presented in Partial Fulfillment of the Requirements

For the Degree of Magisteriate in Arts at

Concordia University

Montréal, Québec, Canada

July 2004

Your file Votre référence
ISBN: 0-612-94632-0
Our file Notre référence
ISBN: 0-612-94632-0

ABSTRACT

Detection of Symmetry and Anti-Symmetry: What they Might Reveal about Visual Nonlinearities

Sandra Mancini

The detection of symmetry and anti-symmetry was investigated by manipulating check size, spatial frequency, grey scale range and eccentricity. Sensitivity to symmetrical stimuli was only modestly affected by these manipulations. The most interesting findings were from anti-symmetrical stimuli. For the anti-symmetrical binary scale stimuli low thresholds were found but these increased to undetectable levels as check size decreased. The high-pass filtering of binary displays only modestly affected performance for anti-symmetrical stimuli; however, the low-pass filtering of these stimuli greatly impaired performance. Increasing the grey scale range of the stimuli led to the undetectability of anti-symmetry. When stimuli with black and white checks were moved from fixation to 8° in the periphery, performance was greatly impaired for anti-symmetrical stimuli. A single model employing a full or half wave rectification would not be able to account for such divergent results.

Acknowledgements

First and foremost, thank you to my supervisor Rick Gurnsey for his patience, understanding and infinite wisdom, and guidance through the years. A special thank you to Sharon Sally, Cindy Potechin and Francois Sezikeye for their useful comments and encouragement. Thank you to other lab members for their moral support. I would also like to thank my thesis committee members: Michael von Grünau, Michael Bross and Rick Gurnsey. Finally, I am thankful to my sister Concetta Mancini and my parents Salvatore and Lucia Mancini for always being there and believing in me. Last but not least I would like to thank Julio Chang.

This research was supported by a grant from NSERC awarded to Rick Gurnsey, and a grant from FCAR awarded to Michael von Grünau and Rick Gurnsey.

Table of Contents

Chapter 1- Introduction

Our ability to recognize objects in the external world seems effortless, yet an elaborate and complex series of processing stages underlies this apparent simplicity. Visual processes are often characterized in terms of lower and higher level stages. Lower level or "early vision" refers to the underlying processes that represent the initial stages of analysis of a visual scene. This is based on the representation of local spatial frequency components. This information is projected beyond the primary visual cortex (V1) and is used in late visual processes. These higher level processes range from the matching of templates to depictions generated from an image.

Texture discrimination is an example of low-level processing because a texture pattern can be accurately represented in area V1 through the output of linear filters tuned to a variety of orientations, positions, spatial scales and phases. The visual system's processing of a texture pattern would be similar to the Fourier decomposition of an image. The neural representation of an image in area V1 is a transformation of an image that preserves all the physical parameters in the image and can be used for further (higher-level) visual processing. Gabor and wavelet filters used in local spatial frequency analysis are examples of filters that preserve all the parameters of an image.

Neuronal networks in higher visual areas compute additional visual properties such as stereoscopic depth and global motion based on the information provided by the output of filters in V1. Processing in most extrastriate and higher visual areas is nonlinear (i.e., the response to complex stimuli is not completely predicted by its response to simple stimuli.)

The perception of symmetry is examined in the present thesis to draw further insight into the visual mechanisms involved in the processing of

symmetrical patterns. It is generally believed that the detection of symmetry is a low-level process. However, the study of symmetry may reveal something about the nonlinearities in visual processing.

1.1 Factors Influencing the Detection of Bilateral Symmetry

A number of aspects of a symmetrical pattern have been manipulated to study the visual system's ability to detect bilateral symmetry. For example, past studies have investigated the role of density (number of elements per unit area) in mirror symmetry detection (Tyler and Hardage, 1996; Rainville, 1999) and both studies found that sensitivity to symmetry was greater for sparse than dense displays.

Another factor that affects symmetry detection is the proximity of information to the axis of symmetry. Barlow and Reeves (1979) and Jenkins (1982) found that sensitivity to symmetry was more affected by the jitter of dots in proximity to the axis of symmetry than dot jitter in the periphery. This suggests that information close to the axis of symmetry is more salient than information further away.

The orientation of the axis of symmetry has also been shown to affect the detectability of symmetry. A number of studies agree that bilateral symmetry is more salient when the axis of symmetry is vertical (Barlow and Reeves, 1979; Corballis and Roldan, 1975; Palmer and Hemenway, 1978; Fisher and Bornstein, 1982; Jenkins, 1983; Pashler, 1990; Wagemans et al., 1992, 1993; Wenderoth, 1994, 1995, 1996a, 1996b). In addition, Corballis and Roldan (1975) found that diagonal symmetries were more salient than horizontal ones. However, this finding was later believed to be the result of an artifact because a line was drawn along the axis of symmetry. In contrast, Wagemans, Van Gool, and d'Ydewalle (1991) found that horizontal symmetries are more

rapidly detected than diagonal symmetries.

The nature of the elements matched across an axis of symmetry has been studied to explore the characteristics that facilitate symmetry perception. Locher and Wagemans (1993) examined the role of element type on symmetry detection. Each of their stimuli contained short lines within a 13 X 13 imaginary grid. The lines composing the patches were either parallel to the axis of symmetry, perpendicular to the axis of symmetry, oblique to the axis of symmetry, or randomly oriented. Sensitivity to symmetry was measured by the reaction time required to decide if the display was random or symmetrical. They found that symmetry detection did not vary as a function of element type. Dakin and Hess (1997) also addressed this question but used a different method than that of Locher and Wagemans. Their stimuli consisted of white noise filtered through horizontal, vertical, or isotropic, spatial frequency selective filters. These three element types were degraded with nine different levels of distortion obtained through phase-randomization technique. Dakin and Hess found that horizontally filtered images (i.e., with oriented "streaks" perpendicular to the axis of symmetry) were more resistant to increasing levels of distortion than vertically filtered images. Horizontal and isotropic filtered images were equivalent.

The contrast polarity of symmetric elements has been investigated by a number of different studies. Patterns comprising symmetric elements that are matched by the same contrast level are considered same polarity stimuli and those matched with "+" or "–" a certain level from mean luminance (i.e. black and white) are defined as opposite polarity stimuli. A pattern comprising black patches matched with black patches is an example of same polarity stimuli and a pattern comprising black patches matched with white

patches is an example of opposite polarity stimuli. The question is whether the visual system is equally sensitive to patterns comprising elements of same polarity and patterns comprising elements that are of opposite polarity. It is generally found that symmetric patterns with opposite polarity matching elements elicit comparable sensitivities as same polarity matching elements when these are presented as isolated kernels (Wenderoth, 1996b; Tyler and Hardage, 1996; Rainville, 1999; Saarinen and Levi, 2000). This issue of contrast polarity will be revisited in a later section.

Barlow and Reeves (1979) generated symmetrical displays along the vertical axis using patterns of dots placed within a circular area. They suggested that symmetry detection requires the comparison of dot densities over a large area. Therefore, the number of comparisons made would be less than the total number of dot pairs since paired regions would be compared instead of single pairs of dots suggesting a global strategy in the detection of symmetry. Similarly, Pintsov (1989) proposed that symmetry detection does not necessitate a point-by-point correspondence between the two halves of a symmetric pattern. Rather clusters of dots from each half of the symmetric display are compared. Pashler (1990) also suggested that symmetry detection operates on grouping principles rather than a point-by-point matching process. Likewise, Wagemans (1993) proposed a local grouping process founded on spatial structures such as proximity or curvilinearity. When observers are presented with dot patterns comprising a symmetrical image, they would rely on local grouping cues such as clusters of dots to detect symmetry. Locher and Wagemans (1993) employed sparse displays comprising line segments of vertical, horizontal or oblique orientations relative to the axis of symmetry. These line segments were positioned in

either a uniform manner (i.e. elements are evenly distributed throughout the display) or a clumping manner (i.e. groups of elements are segregated throughout the display). Subjects were asked to decide as quickly and as accurately as possible whether the stimulus presented was symmetric or random by pressing one of two buttons. They found that for uniformly positioned displays performance was unaffected by the line segment orientation. For displays comprising clumped elements performance was improved when compared to the uniform displays. These results also suggest that local grouping would facilitate symmetry detection.

1.1.1 Symmetry

Points, which are mirror reflected and are matched in terms of position and contrast polarity with respect to a given axis or axes, define the property of bilateral symmetry. An image possessing this property has a perfect positive correlation between corresponding points along a given axis or axes because the points on one side of the axis are mirror reflected with respect to that axis. A "symmetrical" pattern may have symmetrically placed items but not necessarily the property of bilateral symmetry. This is the case when corresponding points are matched in terms of position and not necessarily in contrast. Mirror symmetry is common in the external world. A number of objects found in the visual world are symmetrical (Washburn and Crowe, 1988). For example, both humans and animals have symmetrical faces and bodies. Moreover, plants produce symmetrical leaves and flowers. A number of human artifacts are also symmetric, for example, cars, books and bottles. The ubiquity of symmetry in nature may explain our sensitivity to biological objects and the importance of detecting these in the world. As a result symmetry detection may be involved in object recognition. In many species,

symmetry perception may be a means of survival. For example, symmetry may indicate the presence of a predator or a prey, which would allow an animal to escape or attack. Symmetry perception appears to be effortless (Barlow and Reeves, 1979; Locher and Wagemans, 1993); however, symmetry is a complex image property that seems to be encoded by multiple neural processes (Driver, Baylis, and Rafal, 1992).

There exists a class of visual symmetries and bilateral symmetry is just one type of symmetry. Translations, rotations and reflections in the plane are isometries of the plane and are considered as other types of visual symmetries. These transformations share the following property: the distance between any two points in the original plane is the same as the distance between their images in the transformed plane. However, these other kinds of symmetries are rarely studied because they are much less salient than bilateral symmetry. There are visual symmetries other than mirror symmetry that have been employed in some studies.

Various objects in the visual world are symmetric and their perception generate two images, that is, the original image (IMo) and the image projected on our retina (IMp). The IMp will lose the depth dimension cue and, therefore, many features of one image are now different in the other. This means that the features in the IMp appear different from the features in the IMo, which makes it difficult to connect corresponding points in each image. However, some properties of an image remain unchanged after projection. The more reliable invariant properties (nonaccidental properties) of an image are collinearity, curvilinearity, cotermination, and parallelism. Some metric properties such as length and angle do vary under projection. In many cases bilateral symmetry results in skewed symmetry in the image plane. This

means that bilateral symmetry is projected to skewed symmetry on the retina. Although there is some disagreement on whether skewed symmetry has invariant properties, some believe that skewed symmetry is a nonaccidental property that may be used as a cue to bilateral symmetry (Stevens, 1980; Kanade, 1981; Kanade and Kender, 1983).

1.2 Models of Symmetry Detection

Objects present in the external world are characterized both by luminance differences, that is, first order cues and by texture or contrast differences, that is, second order cues. A number of symmetry models have been derived from various studies in symmetry; some of these models can be broken down into linear and nonlinear processes. The response of a linear mechanism to simple stimuli will predict its response to complex stimuli, whereas the response of a nonlinear mechanism to complex stimuli will not be predicted from its response to simple stimuli. This section reviews models that have been used to detect symmetry including cross-correlation models and computational models. Although these kinds of models have been used to better understand the mechanisms that enable symmetry detection, verbal descriptions have also been important in the understanding of symmetry detection, therefore, a discussion of these will also follow.

Palmer and Hemenway (1978) proposed an early model of symmetry detection that was generally compatible with the historical findings in visual symmetries. From their empirical findings a dual-stage model was derived. The first stage consisted of a crude symmetry analysis by visual inspection in all possible orientations to determine a potential axis of symmetry. Once a reference frame was established in the correct orientation a detailed evaluation of symmetry is performed along the selected axis by comparing the

image on either side of the axis. Figures that are nearly symmetric have small distortions along an axis of symmetry whereas; figures that are rotationally symmetric have halves related by a 180° rotation from the center rather than a mirror reflection. This model accounts for the finding that near and rotational symmetries which are defined as negative symmetries take longer to identify than perfect symmetries. The model also explains the empirical findings for the multiple axis advantage over single axis, which means that it is easier to select an axis of symmetry when there are multiple axes to choose from.

Jenkins (1983) proposed a three-stage model of symmetry detection. This model is based on the capability of the human visual system to detect dense dot textures that have the same orientation and colinear midpoints. The findings in human subjects showed evidence for three sequential processes. The first stage is a process that detects point-pair elements having the same orientations independently of their size. The second stage is the fusing of prominent point-pair elements into a salient image that corresponds to imaginary lines that joint each point-pair element. Finally, the third stage is a process whereby a decision is made whether the salient image is symmetric by putting together the central points of the imaginary lines to determine the orientation of the axis of symmetry. Jenkins data reveal an interesting difference between the second and third stages of the model. The fusion stage is unaffected by the orientation of the axis (vertical or horizontal), whereas the detection of symmetry is better when the axis of symmetry is vertical. He concludes that a V1 representation of bilateral symmetry is not necessary to understand how bilateral symmetric dot patterns are detected.

Good forms in the gestalt sense, which have repetitive and predictable portions, require less information to be processed than a shape without these characteristics. A symmetrical figure would be an example of good form since it is redundant. Zabrodsky and Algom (1994) examined symmetry as a continuous feature. They wanted to quantify the amount of information necessary to detect symmetry by measuring the least effort needed to change a given object into a symmetric object. They measured effort by taking the mean square distances of each point located in a given object to each point located in a symmetric object. They devised a way to evaluate the shape of a figure by obtaining the symmetry distance (SD) of a shape relative to a given visual symmetry (mirror symmetries, translation symmetries, etc.). The information derived from a SD allows the evaluation of different types of symmetries, therefore, comparisons between types of symmetries are possible and statements such as -a shape is more mirror symmetric than rotationally-symmetric- are also possible. There are four steps in obtaining the SD of a shape: (i) get the original shape of a two-dimensional image, (ii) get the normalized shape of the original (i.e. the shape is scaled so that the maximum distance between contour points and the center is the same), (iii) a symmetric shape that best resembles the original shape is obtained based on the SD of that shape, and (iv) obtain the mean squared distance of each point from the normalized image relative to the corresponding point in the transformed figure. The latter step constitutes the SD of a shape. The SD enables the evaluation of any given shape for various kinds of symmetries such as mirror symmetry and rotational symmetry. In addition, the SD also allows the finding of a certain symmetric shape, which is the nearest to a given one. Evaluating the amount of information necessary to see symmetry

will indicate the limitations of a given shape to be perceived as symmetric. In other words, the SD of a shape can help determine how much symmetry information is needed to perceive symmetry in an object.

Jenkins (1983) model is based on first-order relations which consist of orientation uniformity and central point collinearity, however, Wagemans Van Gool, and d'Ydewalle (1991) suggest that second-order regularities between pairs of symmetrical elements are also employed to detect symmetry. Second-order relations are basically geometric regularities between imaginary lines joining point-pair elements. Labonté, Shapira, Cohen, and Faubert (1995) suggested a bilateral symmetry detection model for images comprising dense local features with global symmetry. They reasoned that the first-order strategy is inappropriate for their kind of stimuli (dense global symmetry) because the processing of such stimuli would require larger amounts of computations than random-dot displays like those used in Jenkins (1983) study. Therefore, Labonté et al. (1995) argued that the second-order strategy would be more adequate since detection of global symmetry in dense displays involves the extraction of clusters of local elements that share symmetry relations. In this procedure the grouping of plausible elements is computed prior to symmetry detection. The results of their psychophysical experiments revealed that elements, which are neighboring and similar are grouped together prior to symmetry detection. Based on these findings, Labonté et al. proposed a three-stage strategy for bilateral symmetry detection: (i) *grouping level*: similar local elements are aggregated, (ii) *symmetry-detection level*: symmetrical aggregates are matched according to their axis of symmetry, and (iii) *symmetry-subsumption level*: the axes of symmetry found in (ii) are compared to try to detect global symmetries. During the comparison of

clusters, a certain variation in the orientation and size of the line segment is tolerated. This enables the detection of approximate symmetries. The model's flexibility in terms of being able to resolve non-exact as well as exact symmetries provides an accurate description of the human symmetry perception.

1.2.1 Cross Correlation Models

Cross correlation can be used to determine the extent to which two images match along a given axis. For example, at each point of a symmetric image a comparison can be made between the spatial contents of one side of the axis with its mirror reflected side to determine the degree to which each half match. In this sense, cross correlation is defined as

$$c = \frac{\sum_{j}\sum_{i=1}^{i/2-1} L(i,j) \bullet R(i,j)}{\sqrt{\sum_{j}\sum_{i=1}^{i/2-1} L(i,j)^2 \bullet \sum_{j}\sum_{i=1}^{i/2-1} R(i,j)^2}} \qquad [1]$$

where L (left image) is the vertical reflection of R (right image). The L and R images form each half of a vertically symmetric image.

A fully efficient mechanism is a process that extensively searches through all pairs of elements to find those that are compatible. However, this fully efficient mechanism seems implausible because a considerable amount of uncertainty in the placing of pairs of elements can be tolerated. Therefore, Barlow and Reeves (1979) proposed a model as an alternative to the fully efficient mechanism. This alternative process operates on an area that is sliced into subregions where the numbers of dots in each subregion is computed. If the number of symmetrically placed subregions is equal then the pattern is considered symmetric. However, if the pattern is not symmetric,

the variation in the numbers of dots between two symmetrically placed subregions will be as much as that of any other two regions. This means that the comparison of the absolute number of elements is not as important as the comparison of dot densities to determine whether a pattern is symmetric or not. This would result in a diminished number of comparisons made from all individual dot pairs to the number of paired regions. Barlow and Reeves found that the alternative model gives a reasonable fit to their experimental data, which suggests that symmetry detection in random dot displays would require the comparison of symmetrically placed dot subregions computed over a wide area.

Gurnsey, Herbert and Kenemy (1998) introduced a symmetry model, which supported a low-level processing view of symmetry. Their model involves an initial stage of spatial filtering, followed by a differencing operation and then a second stage of spatial filtering. The differencing operation is a point-by-point dipole - cross-correlation - computation of the image, which would result in a line of zero responses along the axis of symmetry. However, the filtering operation of the second stage represents a computational model employing filtering procedures (these kinds of models are discussed in the following section). The model predicts an increase in symmetry detection as the width of the region increases and as the percent of matching elements along the axis of symmetry increase. If the integration region increases the more likely it is to find matching elements, which make it more likely to detect symmetry when it is present.

1.2.2 Computational Models

Finally, a third class of symmetry models connects the computation of mirror symmetry with low-level mechanisms known to exist in the visual

cortex and is most directly related to the work presented in this thesis. These models will be split into three subsections based on the filtering procedures used to make the computations; the first is phase relationships, the second is frequency content and the third is rectification. An explicit distinction is made between computational models and biologically plausible models. A biologically plausible model involves computations that relate to filters found in V1 and V2 of the visual cortex. In other words, a biologically plausible model is compatible with the known physiology of the visual system. A computational model may explain empirical findings but does not necessarily reflect the physiological processes of the visual system. This means that all biologically plausible models are computational models but not all computational models are biologically plausible. Before reviewing the currently known biologically plausible models, the following section is a brief introduction to the historical development of our understanding of area V1. These findings are the foundations of our understanding of how the visual system processes spatial information.

1.2.2.1 Early Visual Processes

Current understanding of the neural mechanisms mediating spatial vision is heavily influenced by the work related to receptive fields (RFs) of visually responsive neurons. The region on the retina where light changes the firing rate of a cell is called its RF. X-type ganglion cells have either an on/off center-surround or an off/on center-surround and are labeled according to their properties. For example, an on/off center-surround cell has a receptive field that responds with an increase in firing rate when the center of the cell is stimulated by a red light. However, not all cells have the center-surround organization.

X and Y cells differ in important respects. Both cells have center surround RFs, however, X cells have smaller receptive fields than Y cells. In addition, X and Y cells are distributed differently across the retina with considerably more X cells at the fovea and more Y cells in the periphery. Enroth-Cugell and Robson (1966) measured the contrast sensitivity functions of X cells and Y cells by recording the firing rate of each of these cells to a drifting sinewave gratings. They categorized the concentrically organized cells of the retina using stationary and drifting gratings. X and Y cells respond quite differently to a sine wave grating that's drifting across their receptive field - the X fires in tandem with the relative phase of the grating. These cells are said to display linear spatial summation - their response is proportional to the sum of luminance signals coming from all parts of their receptive fields. The Y cell tends to respond to a drifting grating with an overall increase in response that is not dependent on the phase of the stimulus. Y cells therefore respond in a nonlinear manner.

The thalamus is the relay station for sensory information before accessing cortical areas. The lateral geniculate nucleus (LGN) is where the cells in the optic nerve make their first synapses. There are two major subdivisions in the LGN: the magno-cellular (M) layers and parvo-cellular (P) layers with their respective M and P ganglion cell inputs. The Y cells input are only part of the M pathway. In contrast, the X cells input are part of both the P and M pathways. The properties of the parvo-cellular and magno-cellular systems suggest that they are specialized for processing different kinds of input. The parvo-cellular system appears to be specialized to process fine grained patterns and colors, whereas the magno-cellular system appears to be specialized to process gross patterns, and motion (Livingstone and Hubel,

1988).

A number of axons from the LGN neurons project to the primary visual cortex (V1). The retina is retinotopically mapped onto the primary visual cortex. Relative to the retinal size, the fovea is overly represented in the cortex whereas peripheral regions are under represented. This disproportional representation is a natural result of having more receptor cells at the fovea than in the peripheral field.

Hubel and Wiesel (1962) classified cells of the striate cortex as falling into two major categories: simple and complex. Simple cells respond strongly when a stationary stimulus such as a bar is presented within excitatory region of the cell. Complex cells respond weakly or not at all to stationary stimuli. These cells do, however, respond well to moving bars and edges that are correctly oriented.

Like X cells, simple cells encode phase information. Complex cells, like Y cells behave nonlinearly in many different ways (De Valois, Albrecht and Thorell, 1982).

The spatial frequency bandwidth (full width at one-half of peak sensitivity) of striate neurons in the macaque averages about 1.4 octaves and tends to become narrower with increasing spatial frequency (De Valois et al., 1982). Most cortical cells have a preferred orientation, whereas others respond equally well to any orientation. In fact, De Valois and De Valois (1988) found that when cortical cells are broadly tuned for spatial frequency they are also broadly tuned for orientation, likewise cortical cells that are sharply tuned for spatial frequency are also sharply tuned for orientation. De Valois and De Valois showed many cortical cells have RFs that are well modelled by Gabor functions. A Gabor function is obtained by multiplying a sinusoidal grating

with a Gaussian envelope. The V1 cells are filters that break down an image into primitives that can be used to describe a number of other images. These V1 cells generally possess a quasilinear filtering property. In the following subsections biologically plausible models of symmetry detection will be presented.

1.2.2.2 Phase Relationships

Osorio (1996) suggested a simple symmetry sensitive model, which demonstrates that when an image is passed through locally operating filters, the axes of symmetry can be extracted by the categorization of spatial phase. Spatial harmonics can be employed to categorize edges and lines in an image by examining points where harmonics are phase congruent. At the axis of symmetry for example, spatial harmonics are in phase at 90° and 270° which results in a line with no specific contrast. Osorio suggests that symmetry detection is more likely the result of the expertise of a person to recognize objects and not so much the ability to extract information provided by the orientation and position of the elements composing the image. Osorio addressed the detectability of symmetries embedded within a random pattern. Two symmetrical patterns were embedded within a random display. One of the embedded patterns was perfectly symmetrical and the other one was somewhat asymmetrical. Asymmetry was defined as 1 - r, where r is the correlation coefficient of the respective elements comprising the symmetric display. To identify the points of phase congruence (i.e. the axes of symmetry) symmetric and asymmetric patterns were each filtered with two filters. Each pair of filters was two-dimensional Gabor patches of cosine and sine wave grating respectively. One pair of odd and even Gabor filters was smaller and passed high spatial frequency information and the other pair was larger and

passed low spatial frequency information. Filter elements are either symmetric or asymmetric and their collective information can be used to detect a range of spatial frequencies. Points of phase congruence (i.e. along the axis of symmetry) is present when symmetry information is at a local maximum or minimum and anti-symmetry information is close to zero. For a perfectly symmetric patch the model is able to identify many but not all pixels on the axis of symmetry. This can be improved by adding another pair of filters to increase the spatial bandwidth of the mechanism. Osorio found that the axis of symmetry is more often identified for the perfectly symmetrical patterns than for the asymmetrical patterns. The model reveals the importance of local feature detectors, which can make use of the spatial phase information, in the detection of bilateral symmetry.

1.2.2.3 Frequency Content

Rainville and Kingdom (1999) propose a model that combines across spatial channels to predict the detection of symmetrical patterns -first order stimuli- to which white noise was added for different spectral slopes. They investigated whether information in broadband symmetric stimuli would be considered equally at all spatial scales. Their stimuli comprised symmetric broadband noise filtered to $1/f^{\beta}$, where β is the rate of contrast energy decay relative to spatial frequency that ranged from-2 to 5. When stimuli have a $\beta =$ 4, low frequencies dominate, when β = -2, high frequencies dominate and when β = 0, there is an even distribution of spatial frequencies with equal amplitudes. In their stimuli, one of four frequency bands were replaced by phase randomized noise bands, which had center frequencies ranging from 1.7 to 14 cycles per degree such that each notch had a upper and lower cutoff

frequency. When stimuli had $1/f^2$ spectra performance was impaired in practically equal amount at each of the four frequency bands. Stimuli having $1/f^0$ and $1/f^{-2}$ performance was impaired mostly by high frequency noise bands and for stimuli having $1/f^4$ performance was impaired mostly by low frequency noise bands. Their model accurately predicted their human findings, which suggests that information is fused across spatial scales and that symmetry detection benefits equally from information found in broadband symmetric images having constant-octave frequency bands. The latter is valid only if the broadband symmetric images are equated for contrast energy.

1.2.2.4 Rectification

Dakin and Watt (1994) studied four models to determine which aspects of an image are necessary for human symmetry detection. Two of these models employed a blob alignment measure and the other two models employed a correlation measure between the two halves of the image. For each of these two representations (alignment and correlation), two different types of filter (isotropic and oriented) were used. Simulations of the following psychophysical experiments were investigated: the effects of (a) signal-to-noise ratio, (b) positional jitter, and (c) location of symmetry embedded in texture. They found that, when stimuli were filtered with horizontally oriented filters and the alignment measure was employed, results were generally consistent with the human data found by Barlow and Reeves (1979) and Jenkins (1983). However, for both types of filter, the correlation measure of symmetry did not replicate human performance, in many cases the performance of the model was much better than the human performance.

Dakin and Watt suggest that symmetry detection employing the blob alignment measure is part of a broader object recognition process.

Dakin and Hess (1997) employed stimuli that were filtered in the Fourier domain using orientation and scale selective filters. In their psychophysical experiments, patterns were phase-randomized to a range of degrees in order to examine the relative salience of information at different scales and orientations for the detection of symmetry. They found that isotropically as well as horizontally filtered images could tolerate more phase disruption for the detection of vertical bilateral symmetry than vertically filtered images. These psychophysical findings are inconsistent with the model presented by Osorio (1996) who showed that when an image is passed through locally operating filters, the axes of symmetry can be extracted by the categorization of spatial phase. On the other hand, the findings were consistent with Dakin and Watt's (1994) model which measured blob alignment in filtered images. Dakin and Hess proposed two computational models to explain their findings. The quasi-linear model had horizontal and vertical filtering mechanisms followed by a half-wave rectification (all negative values in the convolution output were set to zero) at each of these orientations and the alignment of the elements was measured. The non-linear model had a half-wave rectification (all negative values in the image domain were set to zero) prior to an isotropic filtering followed by a half-wave rectification that was identical to that used in the quasi-linear model. These models provided equally plausible ways of explaining the findings of Dakin and Hess in human subjects for horizontally filtered patterns and isotropically filtered patterns in vertical bilateral symmetry detection. Although the quasi-linear and non-linear models differ in the filtering

sequence, both models seem to suggest that the visual system makes use of half-wave rectification processes to detect vertical bilateral symmetry in patterns that are horizontally or isotropically filtered. For vertically filtered images, the non-linear model is better than the quasi-linear model for low spatial frequencies but generally, both models fail to attain the level of performance achieved by humans.

Rainville and Kingdom's (2000) multi-orientation model of symmetry encoding comprises spatial scale and orientation filters. Their model is built on symmetry-detection units (SDUs), which combine two spatial filters tuned to one of three mirror symmetric orientations (horizontal, vertical or oblique (+/- 45 degrees)). When an axis of symmetry is exactly in-between adjacent filters the SDU response would be zero. In contrast, when the same SDU is placed over non-symmetric sections of the image, filter responses are generally non-zero. To assess symmetry, an image is filtered with vertical, oblique and horizontal SDUs and the responses are full-wave rectified (all negative values in the image domain are set to 1). Finally, a sum is found along the vertical dimension over a chosen height. The multi-orientation model demonstrated that for all three SDU orientations the axis of symmetry could be located in the original image. This model suggests that the visual system computes a full-wave rectification before the axis of symmetry is detected within an image.

Rainville and Kingdom (2002) performed a space-scale analysis of the Fourier and non-Fourier energy content of narrowband symmetrical stimuli with a range of stimulus densities (number of elements per degree). The analysis showed that Fourier energy was present in frequencies higher than 1 cycle per degree (cpd) with a 2.5 cpd centre frequency, whereas non-Fourier

energy was mostly present in frequencies lower than 2 cpd with a tapering off in the higher frequencies. The presence of significant non-Fourier energy at 0.5 cpd was assumed to help in resisting the effects of positional jitter. The space-scale analysis suggests that the available non-Fourier information can only account for the resistance to positional jitter in low-density displays, and not in high-density displays in which case non-Fourier information is not available at greater than 2 cpd, for observers to detect symmetry. However, following a simulation they demonstrated that weak resistance to positional jitter in dense displays is probably the result of a spatial scale selection rather than the inability to make use of the non-Fourier information.

A connection can be made between the notion of rectification and the issue of polarity in symmetry detection but first it is important to realize that a "symmetrical" pattern may have symmetrically placed items but not necessarily the property of bilateral symmetry. The difference between these two properties is that in the latter case the points on one side of the axis are mirror reflected with respect to that axis and in the former case the corresponding points are matched in terms of position and not necessarily in colour. Therefore, the luminance values in an image having perfect bilateral symmetry are perfectly positive correlations across the axis of symmetry. In contrast, an image without bilateral symmetry but with perfectly symmetrically placed items (matched according to position and shape but not colour) would have a correlation < 1 between symmetrically placed items across the axis of symmetry. In some cases the former image, may have a perfect negative correlation when for example, black elements are matched with white elements (and vice versa) across the axis of symmetry. It is suggested in the experimental literature that symmetry (positive correlation)

and anti-symmetry (negative correlation) would have comparable performance levels because after a filter-rectify-filter process is applied to anti-symmetrical stimuli, these have a similar appearance as the symmetrical stimuli. However, the same information content between symmetrical and anti-symmetrical stimuli does not necessarily equal same perceptual sensitivity.

1.3 Symmetry and Polarity Differences

The issue of polarity differences in symmetry detection has been addressed by studying the relative salience of symmetrical and anti-symmetrical stimuli (Masame, 1985; Zhang & Gerbino, 1992; Wenderoth, 1996b; and Saarinen & Levi, 2000). Wenderoth (1996b) employed displays stretching 20 degrees in diameter and comprising 50 dots with each dot having 0.2 degrees visual angle. Participants were asked to discern random displays from those, which contained some degree of symmetry. There were four relevant conditions. The stimuli in each of these conditions comprised both black and white dots except for condition 4 (C4) where only black dots were matching. Condition 1 (C1) had black dots matched with black dots and white dots matched with white dots across a given axis of symmetry. There was a perfect positive correlation between symmetrically positioned dots in C1. Conversely, condition 2 (C2) had black dots matched with white dots and vice versa. For C2 there was a perfect negative correlation between symmetrically positioned dots. Condition 3 (C3) had half of the dots matching in colour (similarly to C1) and half of the dots matching in opposing colour (similarly to C2), which means that there was a zero correlation between symmetrically positioned dots. The axes examined were vertical, horizontal, and left- and right-oblique. After averaging the data over all tested axes, it was

determined that C1, C2 and C3 displays evoke approximately 74%, 70% and 72% correct detection respectively. As for the vertical axis of symmetry only, C1, C2 and C3 displays evoke approximately 80%, 82% and 81% correct detection respectively. These results seem to indicate that the correlation coefficient (0, 1, and -1) between symmetrically placed dots has a weak relationship with the detectability of symmetry. However, after computing the d' for the overall data a slight disadvantage was found for the C2 stimuli when compared to C1 and C3 stimuli and C1 and C4 had similar performance levels.

Using symmetrical and anti-symmetrical stimuli, Saarinen and Levi (2000) investigated whether the orientation of local elements plays a significant role in the global perception of symmetry. The stimuli employed were symmetrical and anti-symmetrical black and white Gaussian blobs. Three conditions were examined: (i) same orientation, in which all tokens were either vertical or horizontal, (ii) mixed matching, in which tokens were both vertical and horizontal, but matched with the same orientation and (iii) mixed opposing, where tokens were both vertical and horizontal, but matched with the orthogonal orientation. The position of the Gaussian blobs centers was reflected to create symmetry. In each display a proportion of these centers were in mirror reflected positions, the rest were randomly positioned. The global symmetric pattern could have 100% (a perfect mirror symmetry image), 75%, 50%, 25% or 0% (no mirror symmetry in the image) of matching elements. They measured the proportion of symmetrical pairs needed to discern mirror symmetry from no symmetry. The threshold represented 84% correct detection. They found that for mixed matching conditions thresholds were comparable or only modestly greater than same orientation conditions

and that mismatched orientations significantly degrade symmetry perception. Levi and Saarinen's control condition consisted of having local dots rather than local Gaussian blobs to form global symmetry. Their findings were consistent with those of Wenderoth who examined C1, C2 and C3 bilateral symmetry -equivalent to same orientation, mismatched orientation, and mixed matching respectively- and found that vertical bilateral symmetry thresholds for C2 and C3 were similar but slightly higher for C1. Their findings revealed that symmetry perception is resistant to differences in local luminance polarity, but not to differences in local orientation cues.

Tyler and Hardage (1996) were also concerned with the detectability of same- and opposite- polarity stimuli. Same polarity stimuli were perfectly symmetric displays and opposite polarity stimuli were perfectly anti-symmetric displays. Their stimuli were generated using black and white Gaussian blobs placed in a grey background. These blobs were either symmetric or anti-symmetric across a vertical axis of symmetry and each of these displays was either dense or sparse. Blobs with sectors to the left or right of fixation were vertically symmetric and those with sectors above or below fixation were horizontally symmetric. For several viewing distances, sensitivity was measured in relation to presentation duration. Sensitivity was defined as the inverse of the exposure duration producing d' = 0.5. The sectors of the stimuli would move further into the periphery as the viewing distance decreased and stimulus size increased. They found that when the symmetric patch was placed at least 2° from fixation, all low-density stimuli elicited similar sensitivities at these eccentricities. In addition, for low-density displays, same- and opposite-polarity stimuli had similar sensitivities. However, in response to high-density stimuli, sensitivity was different

between same- and opposite-polarity for horizontally and vertically symmetric patches. Specifically, in the horizontal sectors, one subject showed lower sensitivity to a symmetric patch of opposite-polarity placed 45° from fixation. Same-polarity stimuli were not affected by the increase in density in the display, but opposite-polarity stimuli were. However, performance for opposite-polarity stimuli did recuperate when stimuli were presented between fixation and 2°.

Similarly, Rainville (1999, chapter 5) found comparable sensitivities to symmetrical and anti-symmetrical stimuli when bandpass, centre-surround micropatterns were presented. Positional jitter was added to each micropattern and performance was measured in relation to this. As positional jitter increased performance declined but detectability remained practically similar for symmetrical and anti-symmetrical stimuli. In line with the results of Tyler and Hardage (1996), when dense displays were presented, performance was more impaired for anti-symmetrical stimuli than symmetrical stimuli.

These studies (Tyler & Hardage, 1996; Wenderoth, 1996b; Rainville, 1999; and Saarineen & Levi, 2000) have demonstrated that the human visual system is equally sensitive to low-density displays comprising symmetrical and anti-symmetrical stimuli. This is in line with the presence of a squaring rectification process in the detection of symmetry. Conversely, when displays were dense, Tyler and Hardage (1996) found that observers were more sensitive to symmetry than anti-symmetry, which conflicts with a universal squaring rectification model.

Cortical processes involved in bilateral symmetry perception can also be examined by studying luminance variations. Often, Gabor filters varying in

orientation and centre spatial frequency, are used to model linear processes. Local variations in luminance are summed based on the information extracted by linear processes. Non-linear processes have initially the same filters as the linear processes but differ in that the output is passed through a squaring or rectification process followed by a filtering stage using Gabor functions and finally an oriented filtering.

Previous studies have shown the importance of luminance in the perception of bilateral symmetry (Wenderoth, 1996b; Zhang and Gerbino, 1992; and van der Zwan, Badcock, and Parkin, 1999). Some of these studies, however, reach different conclusions. Both Zhang and Gerbino (1992) and Wenderoth (1996b) found that symmetry was less detectable in patterns comprising white and black dots placed on either side of the axis of symmetry (C5) than patterns with only black dots matching (C4), but provide different explanations for why this should be. Zhang and Gerbino argue that symmetry detection necessitates a point-by-point comparison of dot pairs differing in contrast. However, Wenderoth suggests that symmetry is dependent on global information rather than on local information. In line with Wenderoth's interpretation, Labonté et al. (1995) showed that the grouping of features on either side of the axes precedes and promotes symmetry detection. Therefore, Wenderoth argues that poor performance with C5 stimuli is probably attributable to the clumping of the dots on each side of the axis, which often leads observers to confuse random displays with symmetric ones (i.e. producing high false alarm rates). In other words, he believes that luminance is a more salient cue than the spatial positioning of the elements. Thus, symmetry detection would be "eclipsed" by luminance grouping of the elements in that clumping would interfere with performance.

The effects of luminance variation can be processed by either an ON or OFF channel. When there is a luminance-increment, information is processed in the ON channel and when there is a luminance-decrement, information is processed in the OFF channel. The question is whether these channels operate within a single mechanism during symmetry perception. Van der Zwan et al. (1999) showed evidence, which suggests that two mechanisms give rise to the percept of symmetry.

Brooks and van der Zwan (2002) examined the effects of luminance in three conditions with single and double axes of symmetry to test the external validity of luminance and polarity based models of symmetry perception. In the equal luminance condition, all dots had the same luminance. In the equiluminance condition, dots were composed of two luminances but matched in luminance across an axis, this condition is the equivalent of C1 in Wenderoth (1996b). The clumping condition employed opposite polarity dots with black dots on one side of the axis and white dots on the other side. The latter condition is similar to Zhang and Gerbino's and Wenderoth's C5. Brooks and van der Zwan measured the mean percentage of correct responses as a function of presentation duration for the three conditions mentioned above. In Experiment 1, they investigated the effect of different luminance levels in the ON channel using luminance-increment patterns. In Experiment 2, they used luminance-decrement to determine whether the processing in the OFF channel would be the same as those in the ON channel. Finally, in the third experiment they examined whether the encoding of information between ON and OFF channels results in a pattern similar to the findings of Experiment 1 and Experiment 2. For all three experiments, they found that performance was similar in the equal and equiluminance

conditions. Performance for the clumping condition was poorer than the other two conditions but symmetry detection was not impossible. This means that clumping does not interfere with the detection of symmetry as Wenderoth suggested because results would have shown a difference in performance between equal and equiluminance conditions, if this were the case. Like van der Zwan et al. (1999), Brooks and van der Zwan also concluded that a dual process better accounts their findings. Nevertheless, there still remains no definite account of the exact mechanisms behind the extraction of structure in a two-dimensional image. This account would give insight into the issue of local versus global information in the detection of symmetry.

1.4 Thesis Objectives

The focus of the present thesis is to further our understanding of the mechanisms involved in the perception of symmetry. The question addressed is whether the human visual system is equally sensitive to symmetrical and anti-symmetrical patterns and what this might reveal about nonlinearities in visual processing. This question was addressed by examining symmetrical and anti-symmetrical images using a novel stimulus. For Experiment 1.1, 1.2, 2.1, 2.2, and 4, stimuli contained black and white checks of varying sizes. The proportion (p) of symmetrically placed dots that were "colour" matched across a vertical axis of symmetry varied from 1 to 0. Figure 1 shows examples of stimuli with different proportions of matching elements across the vertical axis of symmetry. The first column shows stimuli for which p = 1.0, 0.75 and 0.5 in panels (a), (b) and (c) respectively. The second column show stimuli for which p = 0.0, 0.25 and 0.5 in panels (d), (e) and (f) respectively. Examples of symmetrical and anti-symmetrical stimuli are shown in the third and fourth columns respectively. From top to bottom (g-i)

and (j-l), the check sizes are 0.148, 0.296, and 0.594 degrees of visual angle windowed within a circular aperture of 9.5 degrees in diameter.

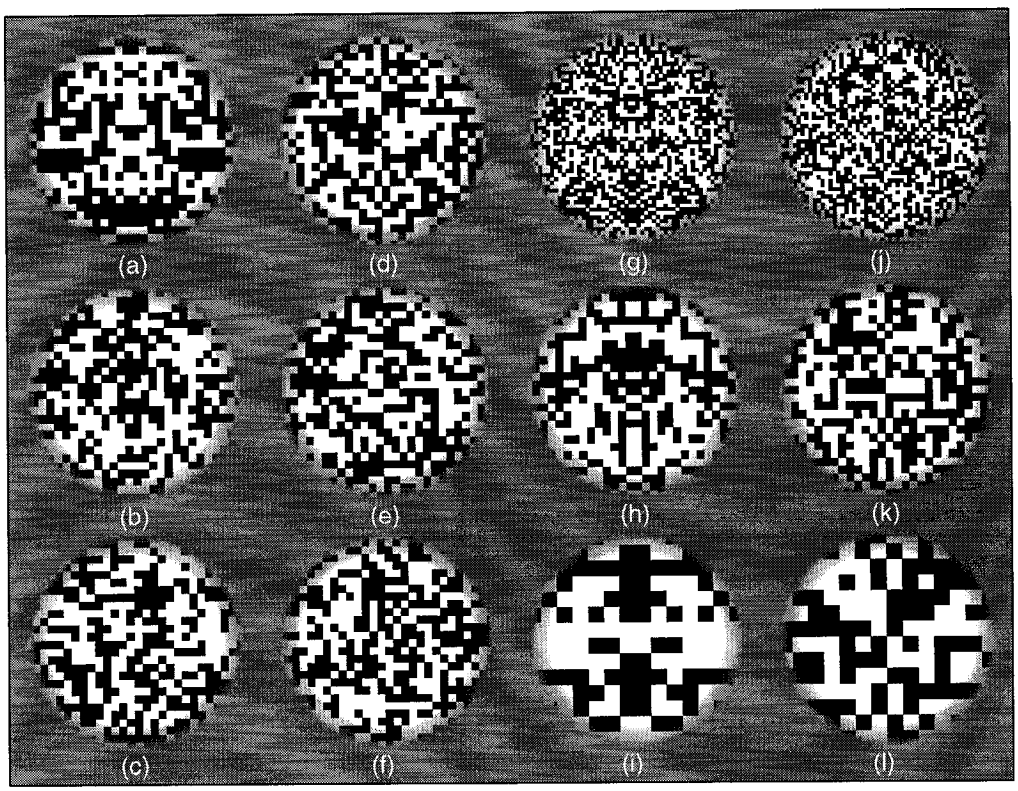

Figure 1. Examples of stimuli with different proportions of matching elements across the vertical axis of symmetry. Pattern in the first column, top to bottom: p = 1.0, 0.75 and 0.5 in panels (a), (b) and (c) respectively; second column, top to bottom: p = 0.0, 0.25 and 0.5 in panels (d), (e) and (f) respectively. Examples of symmetrical (third column) and anti-symmetrical (fourth column) stimuli. From top to bottom, the check sizes are 0.148, 0.296, and 0.594 degrees of visual angle windowed within a circular aperture of 9.5 degrees in diameter.

The stimuli were different from those used previously (Tyler & Hardage, 1996; Wenderoth, 1996b; and Rainville, 1999) because checks comprising the stimuli had no gaps between each other; that is, the entire region of the image was filled with checks of varying size. Therefore, unlike sparse stimuli this kind of stimulus did not provide any positional cues. In addition, stimuli like these can reveal something about the rectification process of the visual system. However, stimuli were more comparable to

those employed by Tyler (1999) and Jenkins (1983).

For experiments 1.1, 1.2, 2.1, 2.2, and 4 in the present thesis, sensitivity is defined as the proportion of polarity matched dots across the axis of symmetry necessary for a pattern to be differentiable from a random display (i.e., $p = 0.5$). Sensitivity was measured by the deviations from $p = 0.5$ needed to achieve threshold accuracy. When p increases from 0.5 to 1 patterns become increasingly symmetrical and when p decreases from 0.5 to 0 patterns become increasingly anti-symmetrical. In order to have sensitivities for symmetry and anti-symmetry stimuli on a same scale, threshold is defined as the absolute difference between p at threshold and $p = 0.5$; $|p_t - 0.5| + 0.5$, where p_t is the proportion of checks matched at threshold. For experiment 3 sensitivity was defined as the stimulus contrast where performance was limited by adding white noise to the symmetrical and anti-symmetrical signals.

The experiments presented in the present thesis will be divided into several chapters. If a full wave or squaring rectification is employed in the detection of symmetry, it is predicted that performance would be comparable for symmetrical and anti-symmetrical stimuli. However, if check size is seen as equivalent to density as defined in Tyler and Hardage (1996) and Rainville (1999) studies, thresholds will be expected to decline as a function of check size for anti-symmetrical patterns. I explore these predictions by examining the effect of check size and aperture. I show in Chapter 2 that for small check sizes symmetrical and anti-symmetrical stimuli have divergent threshold. I examine in Chapter 3 the possibility that symmetrical and anti-symmetrical stimuli are processed by separate mechanisms.

To determine whether the results of Chapter 2 would be generalized to

other types of stimuli, the effects of greyscale range in the perception of symmetrical and anti-symmetrical displays were investigated in Chapter 4.

It has been shown that numerous spatial stimuli differing in scale have similar structure across the visual field (e.g. Watson, 1987; Barrett, Whitaker, & Herbert, 1999; Sally & Gurnsey, 2001). Finally, to investigate the possibility that the findings in Chapter 2 can be replicated in other kinds of manipulations, Chapter 5 addresses the effects of eccentricity in the perception of symmetrical and anti-symmetrical displays.

Chapter 2

2.1 EXPERIMENT 1.1: The Effect of Check Size

Thresholds were measured for symmetry and anti-symmetry stimuli over a range of check sizes. As check size increases the stimuli become less dense, that is, the responses in high-frequency selective spatial filters are fewer. This definition of density would be comparable to that which is used in the Tyler and Hardage (1996) study. One may then predict that for anti-symmetrical stimuli thresholds would decrease as check size increases. However, if a rectification process is underlying the detection of symmetry, symmetrical and anti-symmetrical stimuli may give comparable thresholds across the corresponding check sizes.

METHOD

Participants

Five individuals participated as observers in each of the conditions. Three were experienced psychophysical observers and the other two were naïve to psychophysical testing. Before data collection began, all observers received extensive practice with the present task by completing at least one practice trial for each measured threshold. All observers had normal vision or wore the appropriate corrective lenses during testing.

Apparatus

The experiments were conducted using a Macintosh G4 computer. Stimuli were presented on a 20-inch multiscan colour monitor with display resolution set at 1024 X 768 pixels. Pixel width was 0.37 mm and the screen refresh rate was 85 Hz. The gamma correction software available in the Psychtoolbox (Brainard, 1997) was used to linearize the screen luminance and a Minolta CS-100 photometer was used to find the absolute luminance levels.

Stimuli were created and the experiments were run in the MATLAB (Mathworks Ltd.) environment using functions in the Psychtoolbox (Brainard, 1997) that provide high level access to the routines of the VideoToolbox (Pelli, 1997).

Stimuli

Stimuli comprised black and white checks having widths of 2, 4, 8 and 16 pixels, which from a viewing distance of 57 cm corresponded to 0.074, 0.148, 0.296 and 0.594 degrees of visual angle, respectively. The stimuli were windowed within a circular aperture of 9.5 degrees in diameter. The third column of Figure 1 shows examples of symmetrical stimuli (p = 1.0) having check sizes of 4, 8 and 16 pixels [panels (g), (h) and (i) respectively]. The fourth column of Figure 1 shows examples of anti- symmetrical stimuli (p = 0.0) having check sizes of 4, 8 and 16 pixels [panels (j), (k) and (l) respectively]. The maximum and minimum stimulus luminances were 84.2 and 0.06 cd/m^2.

Procedure

Observers were seated 57 cm away from the screen and were asked to fixate a black dot at the centre of the screen. The fixation dot appeared on the screen only when the stimulus was not present. On each trial two stimuli were presented in succession, one stimulus was completely random and the other had some degree of correlation across the axis of symmetry ($p \neq 0.5$). The subject's task was to determine which interval contained the non-random stimulus. The stimuli were presented for 300 ms and were separated by inter-stimulus interval (ISI) of also 300 ms. The task was, therefore a two-interval forced choice (2IFC) and observers responded by clicking the mouse once or twice to indicate which interval contained the non-random stimulus. Visual feedback after each trial was given in the form of a "+" or "-" to indicate

correct and incorrect responses. An adaptive procedure (PEST, Pentland, 1980) using a Weibull function was used to find thresholds corresponding to 82% correct detections. At least six thresholds were recorded for each observer for each of the eight conditions of the experiment. Two of the subjects had an extra 1 and 2 thresholds recorded.

RESULTS

The left panel of Figure 2 summarizes the results of Experiment 1.1. The threshold data were submitted to a 2 (polarities) by 4 (check sizes) ANOVA. The ANOVA revealed a main effect of size [$F(3,12) = 7.502$, $p < 0.05$], a main effect of polarity [$F(1,4) = 110.167$, $p < 0.05$] and a significant interaction [$F(3,12) = 29.567$, $p < 0.05$]. The main effects of size and polarity and the size x polarity interaction explained, respectively, 65.22, 96.49 and 88.08 percent of the variability among the means. The results show that performance is clearly more dependent on polarity (symmetrical or anti-symmetrical) and size x polarity then check size alone. Symmetrical stimuli elicit thresholds that are relatively unaffected by check size although they do rise moderately as check size increases. Thresholds elicited in response to anti-symmetrical stimuli are extremely high for the smallest check size (indeed, they are essentially unmeasurable). However, as check size increases thresholds drop to a level almost identical to that elicited by the symmetrical stimuli. Given the assumptions about the connection between check size and density in the Tyler and Hardage (1996) paper, these results are generally consistent with theirs. With the exception of the anti-symmetrical small checks, the finding that symmetrical and anti-symmetrical stimuli of larger check sizes have comparable performance levels is consistent with a model using a rectification process such as a filter-rectify-filter model. However, these results

do suggest that symmetrical and anti-symmetrical stimuli are not encoded by the same mechanism across check size.

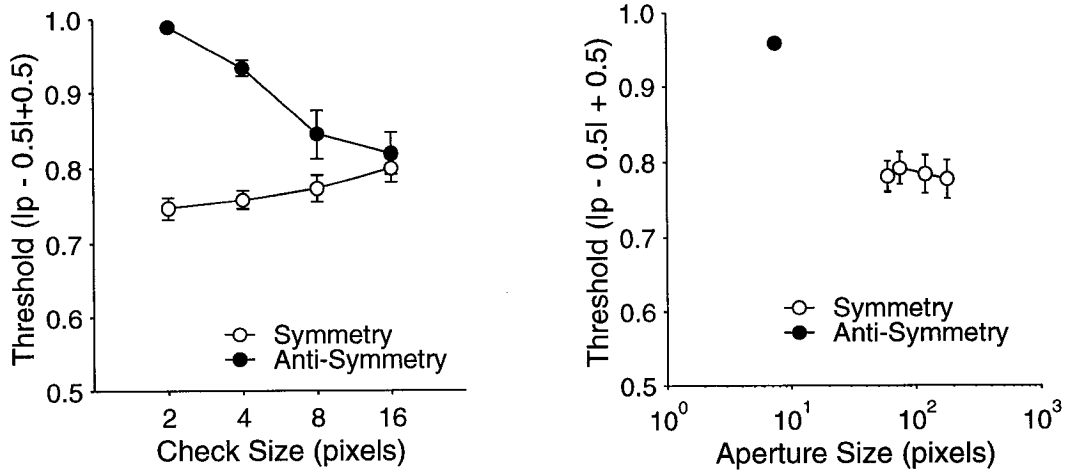

Figure 2. Threshold as a function of check size in pixels for symmetrical stimuli (unfilled circles) and anti-symmetrical stimuli (filled circles). The check sizes were 0.074, 0.148, 0.296 and 0.594 degrees of visual angle windowed within a circular aperture of 9.5 degrees in diameter.

2.2 EXPERIMENT 1.2: The Effect of Aperture Size

In Experiment 1.1, the size of the stimulus window remained fixed across the different check size conditions. This meant that more checks were present in the window containing small checks than large checks. This raises the question of whether the increase in thresholds for the symmetrical stimuli was a direct result of the decrease in the number of checks within the window. Therefore, for symmetrical stimuli in Experiment 1.1 with the largest check size, more trials were conducted at a range of aperture sizes.

Since performance ameliorated for anti-symmetrical stimuli as check size increased, it is possible that a similar issue may have emanated from these conditions. For the smallest check sizes it may be that there were too many responses in the high frequency selective channels that the visual system was flooded with information. To verify whether this was the case, an extra condition for anti-symmetrical stimuli at the smallest check size was tested,

however, the aperture comprised the same number of elements as the largest check size conditions of Experiment 1.1. This means that the aperture size was significantly smaller than that of Experiment 1.1. If the number of responses was not a factor in Experiment 1.1 then this extra condition should also give poor performance.

METHOD

Participants

The participants were the same as in Experiment 1.1.

Apparatus/Procedure/Stimuli

The apparatus and procedure were the same as in Experiment 1.1 with the following exceptions. All symmetrical stimuli comprised checks that were sixteen pixels wide and presented within apertures of 9.5, 11.7, 18.5, & 27.5 degrees of visual angle. The anti-symmetrical stimuli comprised checks that were two pixels wide and presented in an aperture that was 1.18 degrees of visual angle. Five replications of each condition were obtained per observer for each of the five conditions. The reason for having three different aperture sizes for the symmetrical stimuli was to find out whether threshold would increase as more filter responses were added. The filter responses were increased to a maximum comparable to that of the small checks in Experiment 1.1 with an aperture size of 9.5 degrees of visual angle.

RESULTS

The findings are depicted in the right panel of Figure 2. It is clear that decreasing the aperture size for anti-symmetrical stimuli (filled circle) with the smallest check size did not improve performance; thresholds remained very close to 1. It is also clear that increasing the aperture size for the large checks did not improve performance for the symmetrical stimuli. It is safe to

conclude that no aperture effect was operating during the Experiment 1.1 and that changes in the performance level between symmetrical and anti-symmetrical stimuli depend on check size.

Chapter 3

3.1 EXPERIMENT 2.1: High-pass Filtering

The results of Experiment 1.1 seem to indicate the operation of a dual mechanism during the detection of symmetry and anti-symmetry. Since symmetry is easily detectable for all conditions examined in the previous chapter, one can then assume that a mechanism operating uniquely on positive correlations across a given axis of symmetry is present. This mechanism as defined, would obviously be unable to account for the detection of anti-symmetry. Therefore, a reasonable mechanism to explain the low thresholds found for anti-symmetrical large checks of Experiment 1.1, is the operation of a rectification process within the visual system. However, the latter explanation would not account for the dramatic increase in threshold for small check sizes. This would mean that at least two mechanisms are necessary in the detection of symmetry and anti-symmetry.

One is then left to answer the unresolved question of why anti-symmetry is easily detected at large check sizes and not at small check sizes. The answer to this question may be revealed through the examination of the frequency content of the stimuli and the spatial frequencies employed by the processes that detect these stimuli. When the power spectrum of the stimuli is computed, small checks show a flat energy distribution in the Fourier domain whereas large checks show a gradual decrease in energy from low to high frequencies with a greater concentration in the low frequencies (see Figure 3 below). These energy distributions are independent of p.

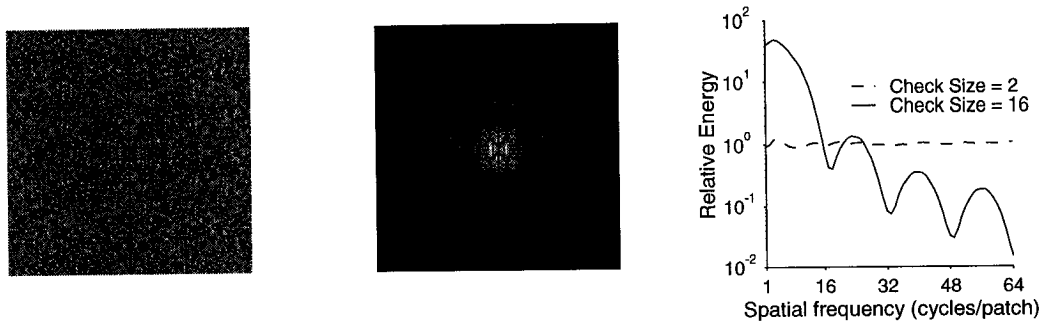

Figure 3. Fourier transformed images and relative energy. Left and center images respectively show the Fourier domain of check size 0.074 and 0.594 degrees of visual angle of anti-symmetrical stimuli. The graph on the right represents the relative energy as a function of spatial frequency for check size 0.074 and 0.594 degrees of visual angle. The graph was obtained by multiplying the Fourier transformed image with 64 filters.

In order to explain the ease, with which anti-symmetrical large check stimuli can be detected, one might suppose that a second mechanism is operating, which involves a full-wave or square-wave rectification of low-frequency selective channels. Thus, a non-linear process would work for low frequencies and a linear process would work for high frequencies with the possibility that the latter channel also operates on low frequencies.

If it is the case that a non-linear channel is operating on low frequencies then thresholds should increase considerably when low frequencies are removed. To verify this possibility, a portion of the stimuli used in Experiment 1.1 was passed through high-pass Butterworth filters to remove low frequencies. A Butterworth filter is a bandpass filter, that is, a filter that lets through a particular band of frequencies (in this case high frequencies) but not those above or below that band (lower frequencies in this case). It is expected that sensitivity to anti-symmetrical stimuli would decrease as more and more low frequencies are eliminated because as it was shown in Figure 3, there is more low frequency information than high frequency information for the large anti-symmetrical checks.

METHOD

Participants

Five individuals participated as observers in each condition. Three of these were also in the preceding experiments. All were experienced psychophysical observers and required little practice. Participants had normal vision or wore the appropriate corrective lenses during the experiment.

Apparatus/Procedure/Stimuli

Sensitivity to symmetrical and anti-symmetrical stimuli of check size sixteen as well as symmetrical stimuli of check size four was measured. All stimuli were passed through Butterworth filters defined as

$$H = 1 / [1 + (c / f)^n], \quad [2]$$

where f is frequency expressed as cycles/patch, c is the cutoff frequency and n is set to 5. Cutoff frequencies of 0, 2, 4, 8, 16, and 24 cycles/patch were used. Because filtering in the frequency domain is equivalent to convolution in the spatial domain, an artifact is produced in the anti-symmetrical stimuli that would make it easily distinguishable from filtered random noise. Specifically, a kernel placed at any position on the axis of symmetry will produce zero response, resulting in a column of zero-crossings along the *axis of anti-symmetry*. To have both symmetric and anti-symmetric zero-crossings perceived equally we reduced contrast along all axes of symmetry and anti-symmetry by multiplying the signal by an inverse Gaussian weighting function

$$G = 1 - \exp(-d / s), \quad [3]$$

where d is distance from the axis of symmetry s = 8 pixels. Examples of high-pass symmetrical and anti-symmetrical stimuli are shown in the first two columns of Figure 4. The left column shows symmetrical stimuli filtered

with cutoff frequencies of 4, 8 and 16 cycles per patch [panels (a), (b) and (c) respectively]. The second column shows anti-symmetrical stimuli filtered with cutoff frequencies of 4, 8 and 16 cycles per patch [panels (d), (e) and (f) respectively]. Thresholds were obtained as before and three replications of each condition were obtained from each subject.

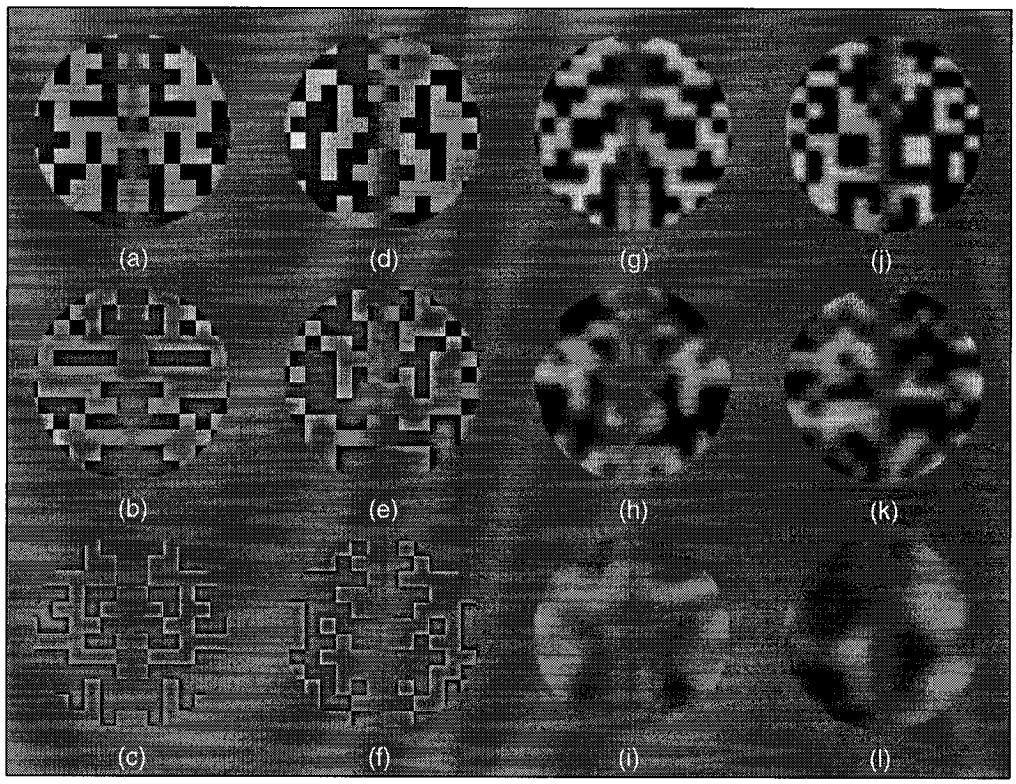

Figure 4. Example of high-passed filtered symmetrical (first column) and anti-symmetrical (second column) stimuli of check size 0.594 degrees of visual angle. From top to bottom, the cutoff frequencies are 4, 8 and 16 cycles/patch in panels a-c and d-e respectively. Examples of low-passed filtered symmetrical (third column) and anti-symmetrical (fourth column) stimuli of check size 0.594. From top to bottom, the cutoff frequencies are 16, 8 and 4 cycles/patch in panels g-i and j-l respectively.

RESULTS

The results of Experiment 2.1 are summarized in the left panel of Figure 5. The results were submitted to a 3 (pattern types) by 6 (filters) within-subjects ANOVA. The ANOVA revealed a main effect of cutoff frequency

[F(5, 20) = 9.785, p < 0.05], which explained 70.98% of the variability in the means. This indicates a general increase in thresholds as more low frequency energy is removed from the display. Although statistically reliable, a 6% increase in threshold from least to most filtering was recorded, which is quite modest in comparison to the effect of check size for the anti-symmetrical stimuli, in Experiment 1.1. There was also a main effect of pattern type [F(2, 8) = 18.294, p < 0.05], which explained 82% of the variability among means. There was no interaction [F(10, 40) = 0.543, p >.05] between pattern type and filtering.

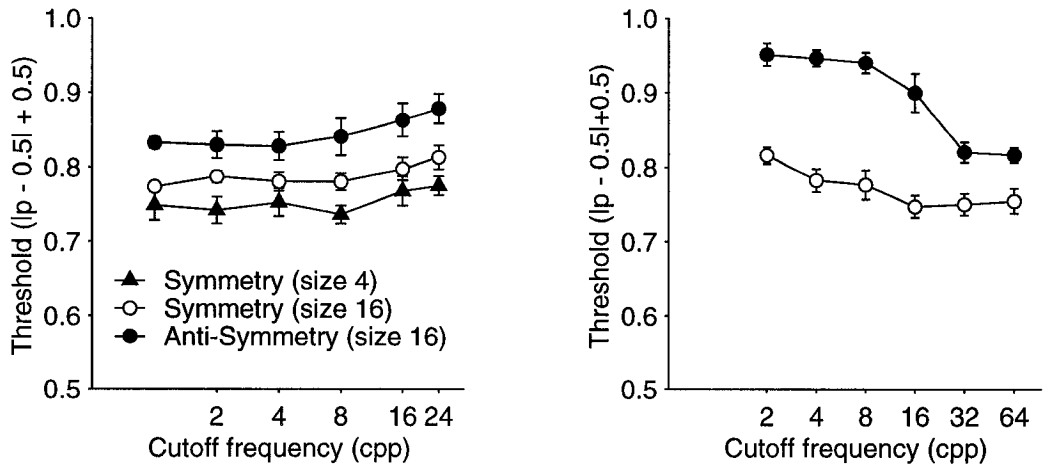

Figure 5. The left graph represents threshold as a function of cutoff frequency for symmetrical checks of 0.148 and 0.594 degrees of visual angle and for anti-symmetrical checks of 0.594 degrees of visual angle. Stimuli were passed through a high-pass Butterworth filter with frequency cutoffs of 0, 2, 4, 8, 16, and 24 cycles/patch. The right graph represents threshold as a function of cutoff frequency for symmetrical and anti-symmetrical checks of 0.594 degrees of visual angle. Stimuli were passed through a low-pass Butterworth filter with frequency cutoffs of 2, 4, 8, 16, 32 and 64 cycles/patch.

Similar to the results recorded for unfiltered stimuli of comparable size in Experiment 1.1, thresholds for filtered stimuli were lower for symmetrical stimuli of check size 4 than symmetrical stimuli of check size 16. However, for the filtered stimuli, participants were less sensitive to the anti-symmetrical stimuli of check size 16 than to the symmetrical stimuli of check

size 16 (see the data on the left of Figure 5). It may be that observers were employing information along the axis of symmetry during discrimination in Experiment 1.1, however, this strategy was no longer available in the present experiment since the axis of symmetry was blurred. Interestingly, removing low frequencies did increase thresholds but not as high as that of the unfiltered smaller check size stimuli of Experiment 1.1. This is further supported by the non-significant interaction between cut-off frequency and pattern type. The low-frequency content of the unfiltered anti-symmetrical stimuli did not seem to help participants in their decision. If anything, it is more likely that observers are using the high frequency information of the unfiltered anti-symmetrical stimuli since observer's sensitivity only slightly decreased as more low frequencies were removed.

3.2 EXPERIMENT 2.2: Low-pass Filtering

Experiment 2.2 compliments Experiment 2.1. The following experiment would allow a direct comparison between the loss of low frequency information and the loss of high frequency information. Rather than putting the stimuli through a high pass filter they were put through low pass filters. If observers were using the high frequency information to discriminate anti-symmetrical stimuli, eliminating these high frequencies should disrupt performance.

METHOD

Participants

Four individuals participated in the experiment. Three of these participated in all of the preceding experiments and one participated in the previous experiment only. All were experienced psychophysical observers who had normal vision or wore the appropriate corrective lenses during

testing.

Apparatus/Procedure/Stimuli

The stimuli were symmetrical and anti-symmetrical stimuli having check size sixteen. The stimuli were passed through a low pass Butterworth filter. The low pass Butterworth filter is define as

$$H = 1 - 1 / [1 + (c / f)^n], \quad [4]$$

where f is frequency expressed as cycles/patch, c is the cutoff frequency and n is an exponent equal to 5. The filters had cutoff frequencies of 2, 4, 8, 16, 32, and 64 cycles/patch. Examples of the low-passed symmetrical and anti-symmetrical stimuli are shown in the right two columns of Figure 4. The third column shows symmetrical stimuli filtered with cutoff frequencies of 16, 8 and 4 cycles/patch [panels (g), (h) and (i) respectively]. The fourth column shows anti-symmetrical stimuli filtered with cutoff frequencies of 16, 8, and 4 cycles/patch [panels (j), (k) and (l)]. Thresholds were obtained as before and three replications per condition were obtained from each subject.

RESULTS

The results are summarized in the right panel of Figure 5. The data were submitted to a 2 (polarities) X 6 (cutoff frequencies) ANOVA. The ANOVA revealed a main effect of cutoff frequency [$F(5, 15) = 10.305$, $p < 0.05$], a main effect of pattern type [$F(1, 3) = 92.224$, $p < 0.05$] and a significant interaction [$F(5, 15) = 3.804$, $p < 0.05$]. The R^2 for cutoff frequency, polarity, and cutoff frequency x polarity respectively revealed that 77.45, 96.85 and 55.91% of the variability is explained by the treatment conditions.

To facilitate a comparison of the effects of removing low and high frequencies from the displays, the check size sixteen data from the left and right panels of Figure 5 were replotted as a function of percent retained energy

(i.e. information retained in terms of spatial frequency) in Figure 6. The figure shows that for symmetrical stimuli detection performance is moderately affected by energy reductions. For symmetrical stimuli there is very little difference in the performance changes for reductions of high and low frequencies. The main difference is in the performance changes for losses of high and low frequencies for the anti-symmetrical stimuli. Performance is clearly more seriously impaired by the loss of high frequencies than by the loss of low frequencies. These findings were unexpected because the energy distributions of anti-symmetrical large checks showed a greater concentration of low frequencies than high frequencies. Therefore, the frequency content of the displays were unable to account for the divergent results between large and small anti-symmetrical checks but still suggest the operation of separate mechanisms during the detection of symmetry and anti-symmetry.

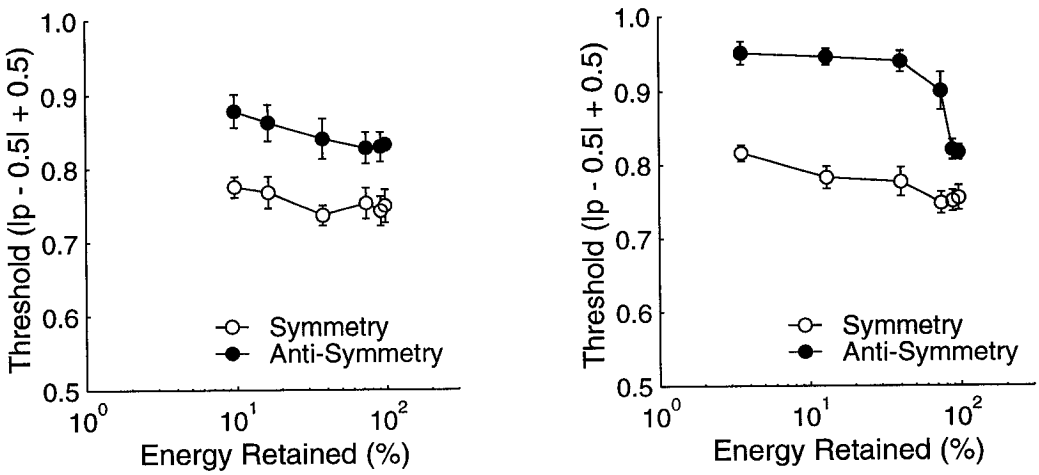

Figure 6. Threshold as a function of *energy retained after filtering* for check size 0.594 degrees of visual angle. Left and right panels represent high-, and low-pass filtered stimuli.

Chapter 4

4.1 EXPERIMENT 3: Greyscale Stimuli

The generality of the results of Experiment 1.1 to other kinds of stimuli was investigated in Experiment 3. The binary checks were replaced by symmetrical and anti-symmetrical stimuli constructed from samples (within 3 standard deviations from the mean) of Gaussian noise. One half of each of these stimuli was generated from samples of zero mean Gaussian noise. The other half of the display was mirror reflected from the original. For anti-symmetrical stimuli, symmetrical checks were sign reversed. Random noise taken from the same distribution was added to limit the performance. The amplitude of the signal, noise and contrast was given by

$$s = \sqrt{c} * signal + \sqrt{1-c} * noise \qquad [5]$$

where c is contrast (which ranges from 0 to 1) and *signal* and *noise* represent the symmetrical (or anti-symmetrical) image and noise components of the display respectively.

METHOD

Participants

Five individuals participated as observers in each of the conditions. All were experienced observers. All observers had normal vision or wore the appropriate corrective lenses during the trials.

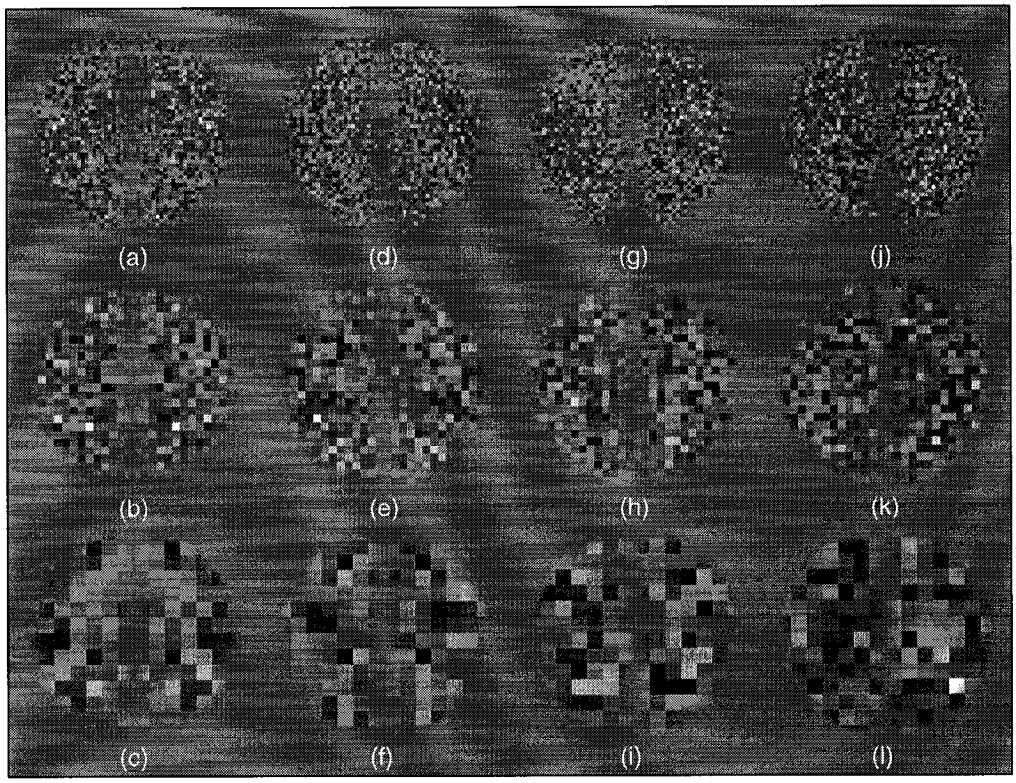

Figure 7. Examples of symmetrical (panels a - f) and anti-symmetrical (panels g - l) greyscale stimuli. The first and third columns were stimuli with c = 1 and second and fourth columns were stimuli with c = 0.8. From top to bottom, the check sizes are 0.148, 0.296, and 0.594 degrees of visual angle windowed within a circular aperture of 9.5 degrees in diameter.

Apparatus/Procedure/Stimuli

Symmetrical and anti-symmetrical displays were created with check-sizes of 2, 4, 8 and 16 pixels. Examples of the stimuli are presented in Figure 7. There is an important difference in the examples shown in figure 7, that is, although the patterns in columns 1 and 3 have c = 1 and patterns in columns 2 and 4 have c = .8, patterns in columns 1 and 2 are both perceived as symmetrical and patterns in columns 3 and 4 are both perceived as random. The apparatus and procedure was exactly as in Experiment 1.1, with the following exceptions. The PEST procedure was replaced by the QUEST procedure (Watson & Pelli, 1983) and stimulus contrast (*c*) was varied rather

than the proportion of matching elements. Both PEST and QUEST procedures are adaptive. However, these differ in the way in which thresholds are obtained; the Quest procedure generally needs fewer trials than the Pest procedure to reach threshold. Three thresholds were obtained in each of the eight conditions for four of the five observers, and one replication was obtained for the remaining subject.

RESULTS

The results are summarized in Figure 8. In many cases thresholds less than one were unobtainable for the anti-symmetrical stimuli. Therefore, for sessions in which QUEST did not converge on a value less than 1, the recorded threshold (contrast) was set to 1. The data were submitted to a 2 (polarities) X 4 (check size) within-subjects ANOVA. The ANOVA revealed a main effect of polarity [$F(1,4) = 142.662$, $p < 0.05$] and no main effect of check size [$F(3,12) = 0.708$, $p > 0.05$] and no interaction [$F(3, 12) = 1.264$, $p > 0.05$]. The R^2 for polarity revealed that 97.23 percent of the variability is explained by this treatment condition.

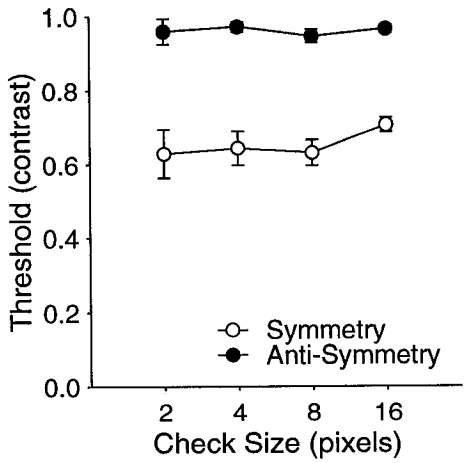

Figure 8. Contrast threshold as a function of check size in pixels for symmetrical stimuli (unfilled circles) and anti-symmetrical stimuli (filled circles). The check sizes were 0.074, 0.148, 0.296 and 0.594 degrees of visual angle windowed within a circular aperture of 9.5 degrees in diameter.

The results of Experiment 3 are quite different from those of Experiment 1.1. The principal difference is that thresholds for anti-symmetrical stimuli do not drop for large check sizes in Figure 8 as they do in the left panel of Figure 2. These results suggest that the ease with which large check size, anti-symmetrical stimuli were detected in Experiment 1.1 has something to do with the limited number of grey scale values in the image rather than with some general second order process, which suggests the operation of separate mechanisms during the detection of symmetry and anti-symmetry. This point is revisited in the General Discussion.

Chapter 5

5.1 EXPERIMENT 4: Eccentricity

There was a substantial difference in thresholds found in Experiment 1.1 and Experiment 3 for anti-symmetrical large check size stimuli, which justifies the further analysis of this discrepancy. As it was discussed earlier information along the axis of symmetry was probably used during symmetry detection in Experiment 1.1 but not in Experiment 2 since contrast along the axis of symmetry was deliberately reduced in the latter. Figure 6 (left and right panels) clearly shows that observers are more sensitive to symmetrical patterns than anti-symmetrical patterns. The data points of check size 16 found in the left panel of Figure 2 correspond to data points of 100% energy retained in Figure 6 because in both situations no energy was eliminated. These results suggest that blurring along the axis of symmetry was responsible for the increase in thresholds. As for Experiment 3, thresholds not only increased but were basically unmeasurable.

Mancini, Gurnsey, and Sally (2003) constructed two ideal observers, which were applied to scaled versions of Figure 1 (binary stimuli used in Experiment 1.1) and Figure 7 (greyscale stimuli used in Experiment 3). These stimuli were passed through $\nabla^2 G$ filters tuned to high frequencies having a σ of 1 pixel (Marr & Hildreth, 1980). One observer was a half-wave rectifier that set all negative values in the output to 0. The second observer was a square-wave rectifier that squared all values in the output. A normalized cross correlation for symmetrically positioned points was computed to measure symmetry (*r*). Each simulated trial involved the convolution of a noise image and 'symmetrical' image, rectification, computation of *r* and selection of the image yielding the highest value of *r* as symmetric. Using the Quest

procedure to vary contrast, ten thresholds were obtained and averaged for each condition (symmetry type by check size). They found that for both scaled versions of Experiment 1.1 and Experiment 3, the square-wave rectifier produced nearly identical sensitivities for symmetrical and anti-symmetrical stimuli at all check sizes. However, the half-wave rectifier was unable to detect anti-symmetry under any condition.

In Mancini et al. (2003) ideal observer analyses emphasize the unresolved issues of Experiment 1.1 and 3. If one believes that a full wave rectification representation of the image is responsible for the ease with which observers detect anti-symmetrical large checks in Experiment 1.1 then this mechanism should give similar findings for that condition in Experiment 3. However, the results of Experiment 3 revealed that anti-symmetrical stimuli are undetectable. This means that a full wave rectification process cannot explain these findings. One is then forced to consider the possibility of a second model since no single model can accommodate both sets of data. For conditions employing blurring along the axis of symmetry, threshold differences between large-check-size symmetrical and anti-symmetrical stimuli seem to indicate that symmetrical and anti-symmetrical stimuli operate under different mechanisms. The latter can be addressed by examining the response to symmetrical and anti-symmetrical stimuli under a different manipulation.

In Experiment 4, large-check-size, symmetrical and anti-symmetrical stimuli were presented across a range of eccentricities to examine whether these conditions would elicit comparable thresholds. It is well known in the literature that various spatial mechanisms, including those involved in the detection of symmetry, have comparable structure across the visual field and

differ only in scale (e.g., Watson, 1987; Barrett, Whitaker, McGraw & Herbert, 1999; Sally & Gurnsey, 2001). If a single channel encodes large-check-size symmetrical and anti-symmetrical stimuli then these should show similar thresholds at fixation and across the visual field when scaling is employed. On the other hand, if results were different this would indicate that more than a single mechanism is involved.

METHOD

The observers, apparatus and methodology were the same as Experiment 1.1. The stimuli were large-check-size (16 pixels) symmetrical and anti-symmetrical. Thresholds were obtained at 0, 1, 2, 4, and 8 degrees of visual angle in the right visual field. Viewing was binocular.

RESULTS

The results of Experiment 4 are summarized in Figure 9. A 2X5 ANOVA was performed on the results and revealed a main effect of eccentricity [$F(4,12) = 48.807$, $p < .05$], a main effect of polarity [$F(1, 3) = 23.324$, $p < .05$] and a trend toward a significant interaction [$F(3, 12) = 2.583$, $p = .09$]. The R^2 for eccentricity, polarity and eccentricity X polarity respectively revealed that 94.23, 88.60 and 46.26 percent of the variability is explained by the treatment conditions. Figure 9 shows that thresholds for symmetrical and anti-symmetrical stimuli increased as a function of increasing eccentricity. Although thresholds for symmetrical and anti-symmetrical stimuli were similar at fixation which would be consistent with a rectification process, they clearly diverged as eccentricity increased. At 8° observers were unable to detect structure in the anti-symmetrical stimuli whereas thresholds for the symmetrical stimuli reached a plateau at $p \approx .86$. These results are clearly inconsistent with the idea that symmetrical and anti-symmetrical stimuli are

encoded by the same mechanism at each eccentricity.

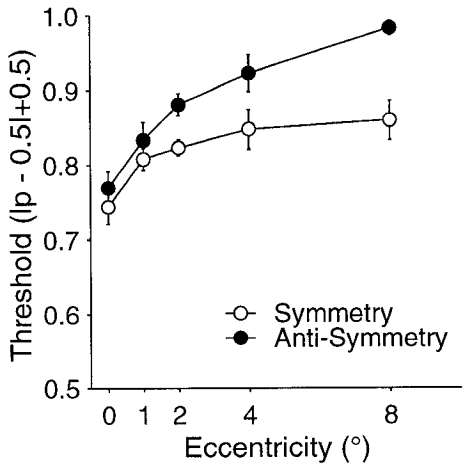

Figure 9. Threshold as a function of eccentricity in degrees visual angle for symmetrical stimuli (unfilled circles) and anti-symmetrical stimuli (filled circles). The check size was 0.594 degrees of visual angle windowed within a circular aperture of 9.5 degrees in diameter.

Chapter 6 – General Discussion

6.1 Overview

The most interesting findings of the present thesis are those involving anti-symmetrical stimuli. In Experiment 1.1, it was found that anti-symmetrical small checks were undetectable, whereas large checks had thresholds comparable to large symmetrical stimuli. For the filtered anti-symmetrical stimuli, thresholds increased as low frequencies and high frequencies were eliminated, however, performance was more impaired by the loss of high frequencies than low frequencies. This suggested that high frequencies are important in the detection of anti-symmetrical stimuli. When investigating whether the findings of Experiment 1.1 were generalizable to greyscale stimuli it was found that anti-symmetrical stimuli were undetectable across check sizes. Finally, when the position of the stimulus along the visual field was manipulated the findings of Experiment 1.1 were replicated; performance was practically unmeasurable as anti-symmetrical large checks were moved further in the periphery.

6.2 Polarity

There is evidence in the literature that symmetrical and anti-symmetrical stimuli have similar performance levels. These stimuli differ uniquely in the polarity of the matching elements and comparable performance levels have been found only when two general conditions were met. The first requirement is the presence of a region that separates each element within the pattern (Wenderoth, 1996b; Tyler & Hardage, 1996; Rainville, 1999; Saarinen & Levi, 2000). The second requirement is that elements have a binary nature, that is, black and white dots (Wenderoth, 1996b), black and white Gaussian blobs (Tyler & Hardage, 1996; Saarinen &

Levi, 2000), on/off center surround micropatterns (Rainville, 1999, chapter 5) or black and white checks (Experiment 1.1). However, for symmetrical stimuli these conditions do not seem necessary since the findings of the present thesis demonstrated only modest changes during the manipulation of check size and spatial frequency content.

The principal goal of the present thesis was to further our understanding of the visual processes behind symmetry detection and the results show evidence for two distinct paths by which symmetry is processed. In one case the mechanism involves the low-level processing of symmetrical patterns and in the other case it involves the processing of the position or "colour" of the elements comprising the anti-symmetrical pattern. The first path would be in line with accepted biological plausible models (Dakin & Watt, 1994; Osorio, 1996; Dakin & Hess, 1997; Gurnsey et al., 1998 and Rainville & Kingdom, 1999, 2000, 2002). Since this mechanism is not affected by various manipulations (e.g. spatial frequency and check size) and does not account for the sensitivity to negative correlations across the axis of symmetry a second process is necessary. The second path would consist of an element by element analysis based on the position or "colour" of the element. In this case density would have an important role, that is, in low-density displays information on element "colour" or element position may be used to correctly detect symmetry. This method of analysis, however, would no longer be appropriate in high-density anti-symmetrical displays where many filter responses are present. As a result, the second mechanism may be operating during the detection of both symmetry and anti-symmetry, whereas the first mechanism could only operate on symmetrical patterns. This dual-process theory would explain the findings of Experiment 1.1 and Experiment

3. Examining the effects of eccentricity in symmetry and anti-symmetry detection in Experiment 4 showed results that further supported the proposed two-mechanism theory.

There are other strategies that can be employed to test the validity of this dual-model theory. For example, the detection of symmetrical and anti-symmetrical patterns may be affected differently when observers are required to split their attention between two tasks (Braun & Julesz, 1998). In this sort of task subjects would be asked to detect symmetry or anti-symmetry while performing a demanding task. Using a 2IFC task, subjects would discriminate a symmetrical pattern from a random one while a shape (e.g. circle, square, or triangle) presented in the center of the pattern would be identified. If a dual path model is operating, performance for the anti-symmetrical patterns should be more impaired by the additional task than performance for the symmetrical patterns.

6.3 Spatial Frequency

The frequency manipulation conducted in Experiment 2.1 and 2.2 is somewhat similar to that of Rainville and Kingdom (1999). In their first experiment they found a U shaped dependence on the degree of contrast energy decay relative to spatial frequency in that symmetry detection was easiest for the frequency range associated with natural images. Consistent results were found when the findings for large symmetrical checks in Experiment 2.1 and 2.2 are combined. Connecting the unfilled circles in the right panel of Figure 5 with the unfilled circles in the left panel of Figure 5 creates an U shaped curve spatial frequency dependence. The U shaped curve derived from connecting the data shows the lowest thresholds for unfiltered stimuli in high-pass and low-pass filtering experiments. The unfiltered

stimuli have most of the energy in the low frequencies as it was demonstrated in Figure 3 which means that the stimuli have a spectra range that resembles more the natural images than not ($\beta > 0$ rather than $\beta < 0$). It must be noted that a direct comparison between Rainville and Kingdom's data and those of the present thesis is difficult because they measured the signal-to-noise ratio between 0 and 1 instead of percent matching between 0.5 and 1

The findings of Experiment 2.1 and 2.2 are also consistent with Rainville and Kingdom (1999) proposed model. The model predicts that information is fused across spatial scales and that symmetry detection benefits equally from information found in constant frequency bands. Comparable thresholds were found for symmetric low-pass and high-pass stimuli which means that symmetry computations are performed across spatial frequency bands.

6.4 Eccentricity

Some of the previous findings on eccentricity have shown an increase in threshold for same size symmetrical stimuli presented in the periphery (Gurnsey, Herbert & Kenemy, 1998; Barrett, Whitaker, McGraw & Herbert, 1999; Sally & Gurnsey, 2001). In contrast, Tyler (1999) found no significant difference between stimuli presented in the periphery and those presented at fixation. Experiment 4 showed a pattern of results for symmetrical stimuli that is not entirely consistent with previous findings, that is, performance gets poorer as the stimulus is moved up to 2° from fixation at which point an asymptotic level is reached.

6.5 Conclusions

The present thesis has shown strong evidence suggesting that

symmetry and anti-symmetry are not processed by a single mechanism. The data reported in the present thesis seem to suggest that the human visual system is not equally sensitive to symmetry and anti-symmetry because these have different performance levels when the following manipulations are studied: check size, spatial frequency content, greyscale range and eccentricity. The use of a single rectification process as was employed in previous studies could not account for all the findings reported in this thesis. Symmetrical stimuli are generally unaffected by the above manipulations which would imply the presence of a low-level rectification process capable of detecting symmetry across different scales. On the other hand, anti-symmetrical stimuli are only detected when elements in the display are sparse and binary in colour. It seems as though the observers compare each item in the display using a selection process rather than a low-level rectification process. This would suggest the use of attentional strategies for the detection of anti-symmetry. To know whether an attentional process is operating during the detection of anti-symmetry future research employing tasks which encompass attentional strategies should be examined. This may reveal something different about the mechanisms underlying the detection of visual nonlinearities.

REFERENCES

Barlow, H. B., & Reeves, B. C. (1979). The versatility and absolute efficiency of detecting mirror symmetry in random dot displays. *Vision Research*, 19, 783-793.

Barrett, B. T., Whitaker, P. V., & Herbert, A. M. (1999). Discriminating mirror symmetry in foveal and extra-foveal vision. *Vision Research*, 39, 3737-3744.

Brainard, D. H. (1997). The psychophysics toolbox. *Spatial Vision*, 10, 443-446.

Braun, J., & Julesz, B. (1998). Withdrawing attention at little or no cost: detection and discrimination tasks. *Perception & Psychophysics*, 60, 1-23.

Brooks, A., & Zwan, R. van der (2002). The role of ON- and OFF-channel processing in the detection of bilateral symmetry. *Perception*, 31, 1061-1072.

Corballis, M.C. & Roldan, C.E. (1975). Detection of symmetry as a function of angular orientation. *Journal of Experimental Psychology: Human Perception & Performance*, 104(1), 221-230.

Dakin, S. C. & Hess, R. F. (1997). The spatial mechanisms mediating symmetry perception. *Vision Research*, 37, 2915-2930.

Dakin, S. C. & Watt, R. J., (1994). Detection of bilateral symmetry using spatial filters. *Spatial Vision*, 8, 393-413.

De Valois, R.L., Albrecht, D.G. & Thorell, L.G. (1982). Spatial frequency selectivity of cells in macaque visual cortex. *Vision Research*, 22, 531-544.

De Valois, R.L & De Valois, K.K. (1988). *Spatial Vision*. Oxford: Oxford University Press.

Driver, J., Baylis, G.C. & Rafal, R.D. (1992). Preserved figure-ground segregation and symmetry perception in visual neglect. *Nature*, 360(6399), 73-75.

Enroth-Cugell, C. & Robson, J.G. (1966). The contrast sensitivity of retinal ganglion cells of the cat. Journal of Physiology, 247, 579-588.

Fisher, C.B. & Bronstein, M.H. (1982). Identification of symmetry: Effects of

stimulus orientation and head position. *Perception & Psychophysics*, 32(5), 443-448.

Gurnsey, R., Herbert, A. M., & Kenemy, J. (1998). Bilateral symmetry embedded in noise is detected accurately only at fixation. *Vision Research*, 38, 3795-3803.

Hubel, D.H. & Wiesel, T.N. (1962). Receptive fields, binocular interaction and functional architecture in the cat's visual cortex. *Journal of Physiology*, 160, 106-154.

Jenkins, B. (1982). Redundancy in the perception of bilateral symmetry in dot textures. *Perception & Psychophysics*, 32(2), 171-177.

Jenkins, B. (1983). Component processes in the perception of bilaterally symmetric dot textures. *Perception & Psychophysics*, 34, 433-440.

Kanade, T. (1981). Recovery of the three-dimensional shape of an object from a single view. *Artificial Intelligence*, 17, 409-460.

Kanade, T. & Kender, J.R. (1983). Mapping image properties into shape constraints: Skewed symmetry, affine-transformable patterns, and the shape-from-texture paradigm. In J.Beck, B. Hope, & A. Rosenfeld (Eds.). *Human and machine vision* (Vol. 1, pp. 237-257). New York: Academic Press.

Labonté, F., Shapira, Y., Cohen, P. & Faubert, J. (1995). A model for global symmetry detection in dense images. *Spatial Vision*, 9(1), 33-55.

Livingstone, M.S. & Hubel, D.H. (1988). Segregation of form, colour, movement and depth: Anatomy, physiology, and perception. *Science*, 240, 740-749.

Locher, P.J. & Wagemans, J. (1993). Effects of element type and spatial grouping on symmetry detection. *Perception*, 22(5), 565-587.

Mancini, S., Gurnsey, R., & Sally, S. L. (2003). Effects of greyscale range on the detection of symmetry and anti-symmetry. Vision Sciences Society, May 2003, Sarasota (Florida).

Marr, D., & Hildreth, E. (1980). Theory of edge detection. *Proceedings of the Royal Society of London B.*, 207, 187-217.

Masame, K. (1985). Perception of symmetry in patterns constructed from two kinds of elements. *Tohoku Psychologica Folia*, 44, 59-65.

Osorio, D. (1996). Symmetry detection by categorization of spatial phase, a model. *Proceedings of the Royal Society of London B.*, 263(1366), 105-110.

Palmer, S.E. & Hemenway, K. (1978). Orientation and symmetry: Effects of multiple, rotational, and near symmetries. *Journal of Experimental Psychology: Human Perception & Performance*, 4(4), 691-702.

Pashler, H. (1990). Coordinate frame for symmetry detection and object recognition. *Journal of Experimental Psychology: Human Perception and Performance*, 16(1), 150-163.

Pelli, D. G. (1997). The VideoToolbox software for visual psychophysics: transforming numbers into movies. *Spatial Vision*, 10, 437-442.

Pentland, A. (1980). Maximum likelihood estimation: the best PEST. *Perception & Psychophysics*, 28, 377-379.

Pintsov, D.A. (1989). Invariant pattern recognition, symmetry, and Radon transforms. *Journal of the Optical Society of America* 6(10), 1544-1554.

Rainville, S. J. M. & Kingdom, F. A. A. (2002). Scale invariance is driven by stimulus density. *Vision Research*, 42, 351-367.

Rainville, S. J. M., & Kingdom, F. A. A. (2000). The functional role of oriented spatial filters in the perception of mirror symmetry–psychophysics and modeling. *Vision Research*, 40, 2621-2644.

Rainville, S. J. M. (1999). The spatial mechanisms mediating the perception of mirror symmetry in human vision. In *Unpublished Ph.D. Thesis*. Montreal, Que., Canada: McGill University.

Rainville, S. J. M., & Kingdom, F. A. A. (1999). Spatial-scale contribution to the detection of mirror symmetry in fractal noise. *Journal of the Optical Society of America A*, 16, 2112-2123.

Saarinen, J., & Levi, D. M. (2000). Perception of mirror symmetry reveals long-range interactions between orientation-selective cortical filters. *Neuroreport*, 11, 2133-2138.

Sally, S., & Gurnsey, R. (2001). Symmetry detection across the visual field. *Spatial Vision*, 14, 217-234.

Stevens, K.A. (1980). *Surface perception from local analysis of texture and*

contour. Cambridge, MA: Massachusetts Institute of Technology, Artificial Intelligence Laboratory.

Tyler, C. W. (1999). Human symmetry detection exhibits reverse eccentricity scaling. *Visual Neuroscience*, 16, 919-922.

Tyler, C. W., & Hardage, L. (1996). Mirror symmetry detection: predominance of second-order pattern processing throughout the visual field. *Human Symmetry Perception*, 157-171.

Wagemans, J. (1993). Skewed symmetry: A nonaccidental property used to perceive visual forms. *Journal of Experimental Psychology: Human Perception and Performance*, 19(2), 364-380.

Wagemans J, Van Gool L, & d'Ydewalle G, (1991). Detection of symmetry in tachistoscopically presented dot patterns: Effects of multiple axes and skewing. *Perception & Psychophysics*, 50, 413-427.)

Wagemans, J., Van Gool, L. & d'Ydewalle, G. (1992). Orientational effects and component processes in symmetry detection. *Quarterly Journal of Experimental Psychology*, 44A, 475-508.

Wagemans, J., Van Gool, L., Swinnen, V. & Van Horebeek, J. (1993). Higher-order structure in regularity detection. *Vision Research*, 33(8), 1067-1088.

Washburn, D.K. & Crowe, D.W. (1988). Symmetries of culture. University of Washington Press, Seattle, WA.

Watson, A. B. (1987). The cortex transform: rapid computation of simulated neural images. *Computer Vision, Graphics, and Image Processing*, 39, 311-327.

Watson, A. B., & Pelli, D. G. (1983). QUEST: a Bayesian adaptive psychometric method. *Perception & Psychophysics*, 33, 113-120.

Wenderoth, P. (1994). The salience of vertical symmetry. *Perception*, 23(2), 221-236.

Wenderoth, P. (1995). The role of pattern outline in bilateral symmetry detection with briefly flashed dot patterns. Special Issue: The Perception of symmetry: II. Empirical aspects. *Spatial Vision*, 9(1), 57-77.

Wenderoth, P. (1996a). The effects of dot pattern parameters and constraints on the relative salience of vertical bilateral symmetry. *Vision Research*, 36(15), 2311-2320.

Wenderoth, P. (1996b). The effects of the contrast polarity of dot-pair partners on the detection of bilateral symmetry. *Perception*, 25, 757-771.

Zabrodsky, H. & Algom, D. (1994). Continuous symmetry: A model for human figural perception. *Spatial Vision*, 8(4), 455-467.

Zhang L., & Gerbino W. (1992). Symmetry in opposite-contrast dot patterns. Perception, 21, supplement 2. 95.

Zwan, R. van der, Badcock, D.R., & Parkin, B. (1999). Global form perception: interactions between luminance and texture information. *Australian, New Zealand Journal of Ophthalmology*, 27, 268-270.